6564–6573 *Nucleic Acids Research, 2016, Vol. 44, No. 14* *Published online 4 July 2016*
doi: 10.1093/nar/gkw589

The use of an artificial nucleotide for polymerase-based recognition of carcinogenic *O*^{6}-alkylguanine DNA adducts

Laura A. Wyss[1,†], Arman Nilforoushan[1,†], David M. Williams[2], Andreas Marx[3] and Shana J. Sturla[1,*]

[1]Department of Health Sciences and Technology, ETH Zu̇rich, 8092 Zürich, Switzerland, [2]Center for Chemical Biology, Department of Chemistry, Krebs Institute, University of Sheffield, Sheffield S3 7HF, UK and [3]Department of Chemistry, Konstanz Research School Chemical Biology, University of Konstanz, 78457 Konstanz, Germany

Received May 20, 2016; Revised June 20, 2016; Accepted June 21, 2016

ABSTRACT

Enzymatic approaches for locating alkylation adducts at single-base resolution in DNA could enable new technologies for understanding carcinogenesis and supporting personalized chemotherapy. Artificial nucleotides that specifically pair with alkylated bases offer a possible strategy for recognition and amplification of adducted DNA, and adduct-templated incorporation of an artificial nucleotide has been demonstrated for a model DNA adduct *O*^{6}-benzylguanine by a DNA polymerase. In this study, DNA adducts of biological relevance, *O*^{6}-methylguanine (*O*^{6}-MeG) and *O*^{6}-carboxymethylguanine (*O*^{6}-CMG), were characterized to be effective templates for the incorporation of benzimidazole-derived 2'-deoxynucleoside-5'-*O*-triphosphates (BenziTP and BIMTP) by an engineered *KlenTaq* DNA polymerase. The enzyme catalyzed specific incorporation of the artificial nucleotide Benzi opposite adducts, with up to 150-fold higher catalytic efficiency for *O*^{6}-MeG over guanine in the template. Furthermore, addition of artificial nucleotide Benzi was required for full-length DNA synthesis during bypass of *O*^{6}-CMG. Selective incorporation of the artificial nucleotide opposite an *O*^{6}-alkylguanine DNA adduct was verified using a novel 2′,3′-dideoxy derivative of BenziTP. The strategy was used to recognize adducts in the presence of excess unmodified DNA. The specific processing of BenziTP opposite biologically relevant *O*^{6}-alkylguanine adducts is characterized herein as a basis for potential future DNA adduct sequencing technologies.

INTRODUCTION

Human genetic material is under constant attack by harmful substances. For example, exposure to alkylating agents from the diet, tobacco smoke, environment, and chemotherapeutics, as well as endogenous sources can lead to DNA damage by chemical alkylation of nucleophilic sites on DNA bases giving rise to DNA adducts (1,2). Among the types of DNA adducts that may be formed, *O*^{6}-alkylguanine (*O*^{6}-alkylG) adducts are of important biological relevance because of their high propensity for inducing mutations (3,4), including G to A transitions prevalent in cancer, for example in codon 12 or 13 of the proto-oncogene K-*ras* (5), and the tumor suppressor gene *p53* (6). Therefore, together with an understanding of the causal relationship between adduct formation and mutagenesis, strategies for locating alkylation adducts in DNA is an important basis to establish early biomarkers of carcinogenesis (7).

Among *O*^{6}-alkylG adducts, *O*^{6}-methylguanine (*O*^{6}-MeG) and *O*^{6}-carboxymethylguanine (*O*^{6}-CMG; Figure 1A) have been found to be present in human blood DNA (8) and tissue samples from meat-eaters and cancer patients (9,10). Putative sources of *O*^{6}-MeG include methylnitrosamines, e.g. the tobacco specific nitrosamine 4-(methylnitrosamino)-1-(3-pyridyl)-1-butanone (11), endogenous methyl donors such as *S*-adenosylmethionine (12), and methylation-inducing antitumor drugs like temozolomide (13). *O*^{6}-CMG is hypothesized to arise from endogenous nitrosation of glycine in the human gastrointestinal tract (14) and its occurrence has been linked to diets high in red meat (10), an established risk factor for colon cancer (15). *O*^{6}-alkylG adducts occur physiologically at extremely low levels and are therefore difficult to detect. Generally applied methods for quantifying *O*^{6}-MeG and *O*^{6}-CMG adducts are based on LC–MS/MS approaches (10,15), however, these methods do not account for DNA

*To whom correspondence should be addressed. Tel: +41 44 632 91 75; Fax +41 44 632 11 23; Email: sturlas@ethz.ch
†These authors contributed equally to the paper as first authors.

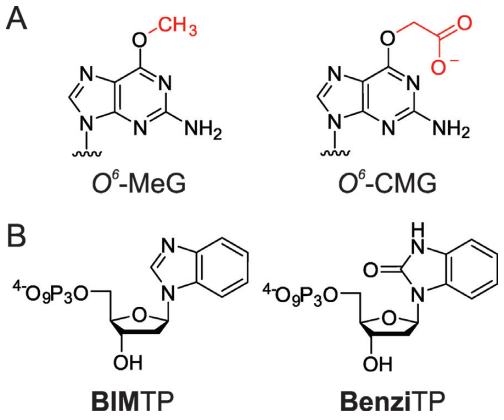

Figure 1. (**A**) Chemical structure of O^6-alkylguanine adducts studied herein. (**B**) Artificial nucleotides **BIM**TP and **Benzi**TP investigated as probes for DNA adducts.

sequence context, nor do they have the potential for amplification of the DNA adduct (16).

Discrimination between various DNA adducts and unmodified DNA with single-base resolution has been achieved by single molecule real time (SMRT) sequencing (17). This approach has excellent potential for future biological applications, but amplification or enrichment of the target sequence is still required prior to sequencing, along with further development of quantitation algorithms. Burrows and co-workers have reported two methods for sequencing oxidative lesions that are substrates for base excision repair (BER) (18,19). Following specific excision of the adducts with BER DNA glycosylases, they either marked the site with an amplifiable unnatural base pair or they identified the adduct location by introducing a deletion mutation (18,19). However, such specific enzymes do not exist for DNA alkylation adducts, thus an alternative strategy could be valuable.

Artificial nucleosides that specifically pair with DNA alkylation adducts together with DNA polymerases with the capacity to process altered base pairs offer a basis for alkylation adduct sensing at single base resolution. Polymerase-mediated incorporation of synthetic triphosphates opposite DNA damage has been reported for abasic sites, isoguanine, 8-oxoguanine (8-oxoG), *cis*-platinated guanine, and O^6-alkylG adducts (20–25). For example, the synthetic nucleoside triphosphate dAdapTP discriminates 8-oxoG from G in single nucleotide incorporation studies by the A-family DNA polymerase *Klenow(exo-)* (22). Artificial bases like **BIM** and **Benzi,** and related analogues in oligonucleotides acted as O^6-alkylG adduct-specific base pairing partners and resulted in the formation of more stable DNA duplexes when paired opposite O^6-alkylG adducts vs unmodified G (26–28). Furthermore, these analogues were polymerase substrates for extending DNA primers terminated with some of the artificial bases paired opposite O^6-alkylG adducts (29,30). Artificial nucleotides **BIM**TP and **Benzi**TP acted as impeding substrates for human DNA polymerase η (h*Pol η*) in replication of the major cisplatin DNA adduct (23). Recently, we communicated specific incorporation of **Benzi**MP opposite O^6-benzylguanine (O^6-BnG) adducts versus nondamaged guanine templates by a mutant *KlenTaq* polymerase *KTqM747K*. Furthermore, **Benzi**TP was required for full-length product formation in bypass of this bulky lesion and additionally was used for amplification of alkylated DNA in linear PCR by *KTqM747K* polymerase (25). This discovery was the first report of an artificial nucleotide being specifically incorporated opposite an O^6-alkylG DNA adduct, but previous studies were carried out with the model adduct O^6-BnG, which has not been observed *in vivo* (31).

Herein, we addressed the scope of an alkylation adduct-artificial nucleotide replication system with regards to O^6-alkylG adducts of biological relevance, namely O^6-MeG and O^6-CMG (Figure 1A). We investigated the bypass of these adducts by a mutant *KlenTaq* DNA polymerase using artificial nucleotides as substrates (Figure 1B). The DNA polymerase *KTqM747K* is a mutant of the N-terminally truncated A-family *Taq* polymerase. It is thermostable and can efficiently bypass various DNA lesions (25,32,33).We found that the O^6-alkylG adducts template the specific incorporation of the artificial nucleotide **Benzi**MP when DNA synthesis was carried out by *KTqM747K*. Furthermore, full-length products were formed following effective incorporation and extension of **Benzi** nucleotide. A 2′,3′-dideoxy **Benzi-**nucleotide was newly synthesized and allowed verification that the artificial nucleotide does not impede *KTqM747K* polymerase in processive DNA replication past natural templates. Furthermore, it enabled marking of the adduct site with the artificial nucleotide. Finally, we found that with **Benzi**TP biologically relevant O^6-alkylG adducts could be recognized in mixtures of damaged and non-damaged DNA. The findings demonstrated herein represent a chemical basis for enzymatic O^6-alkylG adduct detection technologies at single-base resolution that are required for establishing biomarkers of cancer risk or chemotherapeutic drug efficacy.

MATERIALS AND METHODS

Chemical reagents and materials

Reagents were purchased from Sigma-Aldrich and used without further purification. Nucleoside analogues **BIM** and **Benzi** (30,34), and triphosphates **BIM**TP and **Benzi**TP were synthesized as described previously (25). O^6-MeG and unmodified 5'-O-dimethoxytrityl phosphoramidites were purchased from Link Technologies Ltd. The O^6-CMG phosphoramidite was prepared as reported (35). Unlabeled dNTPs were obtained from Invitrogen and [γ-^{32}P]ATP was purchased from PerkinElmer Life Sciences. *KTqM747K* mutant DNA polymerase was kindly provided by myPOLS Biotec GmbH. Pyrophosphatase (Inorganic, *Escherichia coli*) was purchased from New England Biolabs. Silica gel 60 F254 plates with aluminum backing were used for thin layer chromatography. Flash column chromatography was performed on a *Biotage* system with pre-packed Flash+ KP-SiO_2 cartridges. ^{1}H, ^{13}C and ^{31}P NMR spectra were recorded on a Bruker Biospin 400 MHz NMR instrument, and chemical shifts are reported in parts per million (ppm, *δ*) relative to the chemical shift of the respective NMR solvent. High resolution mass spectra were recorded on

Thermo Scientific exactive mass spectrometer with electrospray ionization.

Oligonucleotides

Oligonucleotides were either purchased from Eurofins, Microsynth or Eurogentec. DNA sequences are listed in Supplementary Table S1. Modified oligonucleotides containing O^6-CMG were synthesized as described elsewhere (36). Oligonucleotides were purified by reverse phase HPLC on a Phenomenex Luna C-18 column (5 μm, 4.6×250 mm). The O^6-CMG DNA 28mer was purified with a mobile phase gradient of 10.5–14.5% acetonitrile in 50 mM TEAA over 50 min and eluted at 31 minutes (Supplementary Figures S1 and S2). 48mer O^6-CMG DNA was prepared and purified as reported elsewhere (35). Corresponding oligonucleotide fractions were collected and combined, dried on a centrifugal vacuum concentrator and stored at −20°C until further use. The ssDNA concentration was determined by UV spectroscopy at 260 nm on a NanoDrop 1000 spectrophotometer. Theoretical molar extinction coefficients of the DNA sequences were determined using Integrated DNA technologies online at http://eu.idtdna.com/analyzer/Applications/OligoAnalyzer/.

Primer extension assays

Radioactive labeling of primer strands at their 5' end was carried out using T4 polynucleotide kinase (*Promega*) and [γ-^{32}P] ATP following manufacturer protocol. Primer and templates were annealed by incubating at 95°C for 5 min and slow cooling over 12 h. Final concentrations were 1 μM primer and 1.5 μM template. Standard primer extension reactions (10 μl) contained 1× KTq reaction buffer, 5 nM enzyme, 15 nM DNA (15 nM primer and 22.5 nM template), and 10 μM dNTPs. In full-length DNA synthesis experiments, reactions contained all four natural dNTPs (10 μM total) with or without **Benzi**TP (10 μM). Primer/template, nucleotides and DNA polymerase were incubated at 55°C for 10 min. 1× KTq reaction buffer contained 50 mM Tris–HCl (pH 9.2), 16 mM $(NH_4)_2SO_4$, 2.5 mM $MgCl_2$, and 0.1% Tween 20. Reactions were quenched by adding 20 μl PAGE gel loading buffer (80% formamide, 20 mM EDTA, 0.05% bromophenol blue, 0.05% xylene cyanole FF) and the product mixtures were analyzed by 15% polyacrylamide/7M urea denaturing gels and subjected to autoradiography (Bio-Rad). Quantification was carried out with Bio-Rad Quantity One software.

Steady-state kinetic analysis

Steady-state kinetics parameters for single nucleotide incorporation by DNA polymerase *KTqM747K* were determined under single completed hit conditions (37,38). For various dNTP concentrations, the quantity of $n+1$ product formed by performing the reaction at 55°C was measured. Reaction mixtures included 5 nM enzyme, 100 nM primer, 150 nM template, and 1× KTq reaction buffer. Reactions were initiated by adding pre-warmed enzyme and DNA mix to pre-warmed dNTPs. Reactions were quenched by adding PAGE loading buffer. Products were separated on a 15% polyacrylamide/7M urea denaturing gel, visualized by autoradiography, and quantified with Quantity One Software (Bio-Rad). To obtain kinetic parameters v_{max}, K_M and k_{cat}, the intensities of $n+1$ bands (quantified on the Quantity One Software, Bio-Rad) were fit to a Michaelis–Menten rectangular hyperbola using SigmaPlot12 Software (Systat Software). Reactions were performed in triplicate and for K_M values, means (± standard deviations) are reported.

Linear amplification of O^6-alkylG DNA

Reactions were incubated in a Biometra T3000 thermocycler, where 30 cycles of denaturation, annealing, and elongation were performed under the following conditions: 30 s at 95°C, 30 s at 42°C, and 30 s at 55°C. Reactions contained 0.5 ng of corresponding O^6-alkylG template DNA (28 nt), 300 nM primer (19 nt), 25 nM *KTqM747K* DNA polymerase, 1× KTq reaction buffer, all four dNTPs (10 μM), and 10 μM or no **Benzi**TP. Product mixtures were separated on a 20% polyacrylamide/7M urea denaturing gel, stained with SybrGold nucleic acid gel stain (Invitrogen) and visualized on a Bio-Rad molecular imager Gel Doc XR+ Imaging System. Product bands were quantified using the software Image Lab 3.0 (Bio-Rad) and normalized to the known quantity of the 28 nt marker loaded on the same gel, indicating a yield of 14.6 ng amplicon (theoretical yield on the basis of 30 cycles is 15 ng).

Molecular modeling studies

Structures were computed with the Molecular Operating Environment software suite (Chemical Computing Group). Crystal structures of a *KTq* mutant polymerase with incoming ddCTP opposite template G (PDB code: 3PY8) (33) and structures of *Bst* DNA polymerase with incoming dCTP opposite template G (PDB code: 1LV5) or incoming ddTTP opposite template O^6-MeG (PDB code: 2HHW) were used (39). For modeling studies with the *KTq* mutant, crystal structure (PDB code: 3PY8) was modified by attaching an O^6-CMG group to the templating G and replacing incoming ddCTP by **Benzi**TP or **BIM**TP (in favored *syn* conformation). In studies involving *Bst* DNA polymerase with template G incoming dCTP (PDB code: 1LV5) was replaced by *syn* **Benzi**TP and for template O^6-MeG, dTTP was altered to *syn* **Benzi**TP (PDB code: 2HHW). For energy minimizations the potential energy of the protein was fixed and followed by applying the Amber99 force field. Visualization was performed in the PyMol software (Schrodinger).

Application of ddBenziTP to mark O^6-CMG adducts in DNA

The same protocol was followed as described for primer extension reactions. dd**Benzi**TP was added at increasing concentrations (0, 100, 500, 1000 and 2000 μM) to all four natural dNTPs (10 μM) and **Benzi**TP (10 μM). Reaction mixtures (10 μl) contained 1x KTq reaction buffer, 5 nM *KTqM747K* DNA polymerase, 15 nM DNA (15 nM radioactively labeled primer annealed to 22.5 nM template), and 1/60 units pyrophosphatase, and were allowed to react at 55°C for 10 min. Reactions were quenched by adding 20 μl PAGE gel loading buffer, and analyzed by separating on

15% polyacrylamide/7M urea denaturing gels and visualized by autoradiography (Bio-Rad).

Sensing O^6-alkylG-containing DNA mixed with unmodified DNA

Mixtures of G and O^6-alkylG DNA were prepared with a constant amount of template (22.5 nM template annealed to 15 nM radiolabeled primer) at varying ratios of G:O^6-alkylG DNA: 1:0, 1000:1, 100:1, 10:1, 5:1, 3:1, 2:1, 1:1. Primer extension reaction mixtures (10 μl) contained 1× KTq reaction buffer, 5 nM enzyme, 15 nM DNA, and 10 μM **Benzi**TP. DNA mixtures were prewarmed and **Benzi**TP/Polymerase mixture was added and allowed to react at 55°C for 10 min. Products were separated on a 15% polyacrylamide/7M urea denaturing gel and visualized by autoradiography. Intensity of $n + 1$ bands was quantified on the Quantity One Software (Bio-Rad). The experiment was performed in triplicate and mean values ± standard deviations are reported.

RESULTS AND DISCUSSION

Translesion DNA synthesis past O^6-alkylG adducts by *KTqM747K*

To investigate the capacity of the mutant *KlenTaq* polymerase *KTqM747K* to replicate DNA containing O^6-MeG or O^6−CMG, primer extension studies were performed. Thus, a 5'-end radiolabeled 23 nucleotide (nt) primer and a 28 nt template containing either G, O^6-MeG, or O^6-CMG (referring to X positioned at nucleotide 24, Figure 2A) were allowed to react with *KTqM747K* polymerase and dNTPs, (Figure 2). Extension products were analyzed by gel shift assay on denaturing polyacrylamide gels and visualized by autoradiography. For results presented in Figure 2, the level of nucleotide incorporation is indicated as percent primer extension and was calculated as a ratio of the amount of $n + 1$ extension product formed to initial amount of primer.

The capacity of *KTqM747K* to replicate DNA containing O^6-alkylG adducts in the presence of four natural dNTPs depended on adduct structure. Replication in the presence of O^6-MeG gave rise to full-length product (26%, Figure 2B, X = O^6-MeG, lane 4), whereas in the presence of O^6-CMG significantly less full-length product was observed (7%, Figure 2B, X = O^6-CMG, lane 4). In both cases, misincorporation of dTMP was favored over correct dCMP incorporation (Figure 2B). For O^6-MeG, dTMP was incorporated to a large extent (92%) and dCMP was also incorporated (41%). For O^6-CMG templates, natural nucleotides were incorporated less than they were for O^6-MeG templates. Thus, there was 32% dTMP misincorporation and 17% correct dCMP incorporation. In a previous study concerning O^6-BnG (25), the polymerase was stalled. Considering the proficiency of O^6-MeG bypass, stalling in the other two cases may be attributed to the larger sizes of the adducts. For O^6-BnG, dTMP misincorporation was favored over dCTP incorporation (32 vs 18%) (25). Misincorporation of dTMP has been observed in bypass of O^6-MeG by bacterial *Escherichia coli KF* DNA polymerase (40), *B. stearothermophilus Bst* polymerase, *Vent (exo-)* (41), viral

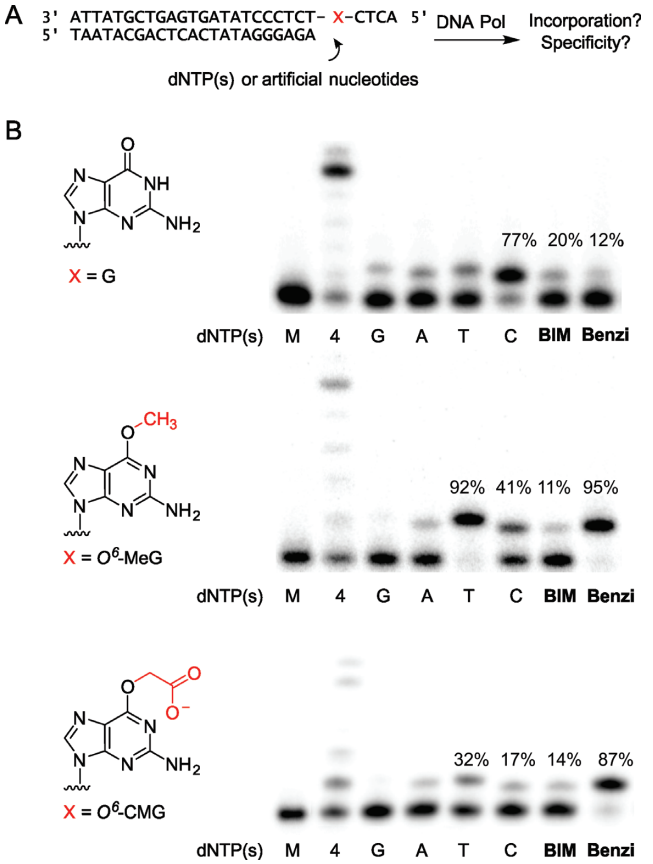

Figure 2. (**A**) DNA polymerase-mediated primer extension experiments and sequences used in this study. (**B**) Replication by *KTqM747K* DNA polymerase past templates with X = G, O^6-MeG, or O^6-CMG for natural or artificial nucleotides. M, blank; 4, all four dNTPs; G, dGTP, A, dATP, T, dTTP; C, dCTP, **BIM**, **BIM**TP; **Benzi**, **Benzi**TP; final dNTP concentrations were 10 μM or 10 μM each in case of 4, incubated at 55°C for 10 min.

T4 (42), *T7 (exo-)* DNA polymerase and HIV reverse transcriptase (43), or eukaryotic *Drosophila melanogaster Pol α* (44). Also, human *Pol β* and translesion *Pol ι* had a similar preference for dTTP when replicating over O^6-MeG (4,45).

Specific incorporation of an artificial nucleotide opposite O^6-alkylG DNA adducts

Having established how *KTqM747K* polymerase bypasses O^6-alkylG adducts with natural nucleotides as substrates, the incorporation of two benzimidazole-derived base-modified nucleotide analogues (**BIM**TP and **Benzi**TP) was investigated in the same manner as described above, adding **BIM**TP or **Benzi**TP in primer extension reactions. Both artificial nucleotides were effective substrates for *KTqM747K* polymerase (Figure 2B). However, **BIM**TP yielded little extension product in general: G (20%), O^6-MeG (11%), and O^6-CMG (14%; Figure 2B). On the other hand, **Benzi**TP was a good substrate and there were high incorporation percentages for both adducts (Figure 2B, X = O^6-MeG: 95%; X = O^6-CMG: 87%) but, importantly, not with G (Figure 2B, X = G: 12%). This observation matched the preference for alkylated templates previously reported for O^6-

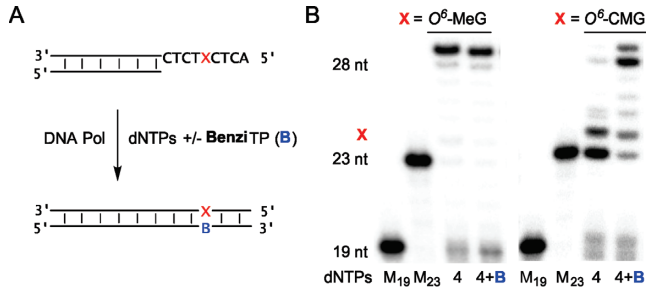

Figure 3. Full-length product formation in replication of O^6-alkylguanine adducts by *KTqM747K*. (**A**) Setup of running start primer extension experiment. (**B**) PAGE analysis of 19 nt primer extension products with template X = O^6-MeG or O^6-CMG at position 24 nt. M_{19}, marker for primer (19 nt); M23, marker for 23 nt (position prior to adduct site X) 4, all four dNTPs (10 μM); 4+**B**, all four dNTPs (10 μM) plus 10 μM **Benzi**TP.

BnG (25). Since natural nucleotides also were incorporated readily under the standard reaction conditions (55°C, 10 min) when O^6-MeG was in the template, conditions were adjusted to improve selectivity for **Benzi**TP over natural dNTPs in the case of O^6-MeG (SI, Figure S3). By carrying out the reaction at 72°C for 2 min, incorporation of natural nucleotides was dramatically reduced (25% dTTP, 6% dCTP), whereas **Benzi**MP incorporation resulted in 80% extension product and only 4% incorporation opposite G. In summary, **Benzi**MP was specifically incorporated opposite O^6-alkyl-G and DNA adducts over G.

To investigate the influence of the bases flanking the DNA adduct in this process, we studied two alternative sequences besides –CXT- with O^6-CMG at position X (SI, Figures S4 and S5). In one sequence, we changed the 5' pyrimidine to a purine (-GXT-) and in the second, the 3' T was replaced by a C (-GXC-). In both cases, **Benzi**TP was favored as a substrate over natural dNTPs when O^6-CMG was in the template. Furthermore, full-length products were formed to a significantly higher extent in the presence of all four natural dNTPs plus **Benzi**TP than in reactions without **Benzi**TP (SI, Figures S4 and S5; <10% full-length product with 4 dNTPs only vs up to 50% full-length product in presence of 4 dNTPs plus **Benzi**TP).

Artificial nucleotide is required for efficient full-length DNA synthesis of O^6-CMG templates

Knowing that **Benzi**MP is efficiently incorporated opposite O^6-alkylG adducts, we characterized how the artificial nucleotide impacted full-length DNA synthesis in lesion bypass. Thus, we examined whether a 19 nt primer could be elongated if the template contained O^6-alkylG five bases downstream from the primer terminus (at nt 24) in the presence of all four natural dNTPs and **Benzi**TP (Figure 3). The O^6-MeG adduct was readily bypassed by *KTqM747K* polymerase and full-length products (over 90%) were formed with natural dNTPs only or with supplemented **Benzi**TP (Figure 3B, X = O^6-MeG). However, when O^6-CMG was in the template, replication was stalled (Figure 3B, X = O^6-CMG, lane 4. Bands at 23 nt and at adduct site X, 24 nt). The addition of **Benzi**TP significantly promoted the formation of full-length products in in this case. With both alkylated templates, a prominent band at 29 nt was visible, likely due to template-independent incorporation of an additional nucleotide (46). **Benzi**TP was required for efficient bypass of O^6-CMG by overcoming the stalling of the polymerase at the adduct site to result in full-length products.

Steady-state kinetic analysis of translesion DNA synthesis

In order to quantitatively compare efficiencies of nucleotide incorporation in replication of DNA containing O^6-MeG or O^6-CMG, steady-state kinetic parameters for *KTqM747K* polymerase catalysis were determined (Table 1). In this experiment, single nucleotide incorporation (*n+1* product formation) was followed over time, and kinetic parameters K_M and k_{cat} were derived (37). In general, the presence of the O^6-alkylG DNA adducts did not greatly influence the catalytic turnover k_{cat}, but decreased the binding affinity (increasing K_M) compared to replication of unmodified DNA with natural dNTPs. The catalytic efficiencies k_{cat}/K_M for synthesis past O^6-MeG (0.038 $\mu M^{-1}min^{-1}$), O^6-CMG (0.007 $\mu M^{-1}min^{-1}$), and O^6-BnG (0.021 $\mu M^{-1}min^{-1}$) (25) by *KTqM747K* were similar to values measured previously for incorporation of dTMP opposite O^6-MeG by the A-family *Bst* DNA polymerase (0.075 μM^{-1} min^{-1}) (39). Compared to misincorporation of dTMP by the archaeal *Sulfolobus solfataricus* DNA polymerase *Dpo4* (dTTP opposite O^6-MeG: 0.0044 μM^{-1} min^{-1}) (47), the *KTqM747K* polymerase tested herein was 9-fold more efficient in replicating O^6-MeG adducts. The human translesion DNA polymerase η on the other hand is more efficient in translesion synthesis past O^6-alkylG adducts than *KTqM747K*: 20-fold more for O^6-MeG (48), and 9-fold more in bypass of O^6-CMG (35).

The K_M value for processing of **Benzi**TP was the same order of magnitude for unmodified as well as adducted templates (Table 1). However, catalytic turnover k_{cat} was significantly higher for replication over O^6-alkylG adducts versus G (17-fold for O^6-CMG; 55-fold for O^6-MeG). The highest catalytic efficiency k_{cat}/K_M for **Benzi**MP incorporation was observed when O^6-MeG was in the template, and was 13-fold higher than for O^6-CMG or 6-fold than for O^6-BnG (k_{cat}/K_M 0.120 $\mu M^{-1}min^{-1}$) (25). Finally, by comparing these values with catalytic efficiencies for incorporation of **Benzi**MP opposite natural templates (25), incorporation opposite A was almost 2-fold more efficient than with templating O^6-MeG. However, processing of **Benzi**TP opposite A was 30-fold less efficient than incorporaton of dTMP (25). When comparing incorporation of **Benzi**MP vs dTMP, the difference in selectivity was 19-fold with the O^6-MeG template, 8-fold for O^6-CMG, and 6-fold for O^6-BnG (25). We previously demonstrated that **Benzi**MP was also incorporated by *hPol η* during replication of unmodified or platinated G templates (23). However, incorporation of **Benzi**MP by *KTqM747K* opposite O^6-MeG was 29-fold more efficient than its incorporation by *hPol η* opposite the major platinum intrastrand cross-link product *cis*-Pt-1,2-d(GpG) (k_{cat}/K_M 0.025 $\mu M^{-1}min^{-1}$) (23). In summary, kinetic data confirmed the specific incorporation of **Benzi**MP opposite O^6-alkylG adducts compared to guanine with the catalytic efficiency of incorporation opposite G being reduced 150-fold compared to O^6-MeG, 24-fold for O^6-BnG (25), and 12-fold for O^6-CMG. Steady-state kinetic data re-

Table 1. Steady-state kinetic parameters for nucleotide incorporation by *KTqM747K* DNA polymerase

dNTP	K_M [μM]	k_{cat} [min^{-1}]	k_{cat}/K_M [$\mu M^{-1}min^{-1}$]
X = G			
dCTP	0.07 ± 0.02	14	190
BenziTP	48 ± 8	0.24	0.005
X = O⁶-CMG			
dTTP	519 ± 54	3.6	0.007
BenziTP	70 ± 10	4.06	0.058
X = O⁶-MeG			
dTTP	410 ± 66	15.6	0.038
BenziTP	18 ± 4	13.2	0.730

vealed the fastest incorporation efficiencies for **Benzi** were opposite O^6-MeG, and the highest selectivity for **Benzi**TP over natural dNTPs was observed for O^6-MeG templates. Findings from primer extension and steady-state kinetic experiments indicate that *KTqM747K* polymerase can readily bypass O^6-MeG, with natural nucleotides being well incorporated. Since *KTqM747K* was significantly stalled by O^6-CMG and adding **Benzi**TP promoted bypass of this adduct, we focused further attention on O^6-CMG.

Molecular modeling of O^6-CMG: Benzi base pair

Molecular modeling was performed to visualize a possible structural basis for the specific incorporation of **Benzi** opposite O^6-CMG. Thus, molecular mechanics simulations of base pairing interactions between **Benzi**TP and G or O^6-CMG in the active site of a *KlenTaq* mutant polymerase (I614K, M747K; PDB code: 3PY8) (33) were performed. Original crystal structures containing an incoming ddCTP opposite templating G were modified by replacing ddCTP with **Benzi**TP and adding a carboxymethyl group to the templating G. The modified nucleotides were placed in *anti* conformation, since in *syn* conformation a steric clash was evident between the substituent at position 2 on the nucleobase and the oxygen of the sugar moiety (23). Following energy minimization (Amber 99 force field, Figure 4 and SI, Figure S6) possible differences in base pair geometries were considered. For incoming **Benzi**TP in the *KTq* mutant active site **Benzi**TP was computed to be flipped out when paired with G (Figure 4A). Whereas **Benzi**:O^6-CMG was predicted to adopt a planar Watson-Crick-like geometry and potentially form two hydrogen bonds (Figure 4B): one between the –NH donor on **Benzi** and the N2 of O^6-CMG (2.4 Å); the other was predicted between the carbonyl group of **Benzi** and the –NH2 donor on O^6-CMG (2.1 Å). Similar findings were observed with *hPol η* in replication of the major cisplatin adduct where two hydrogen bonds were possibly formed with **Benzi** when it was incorporated opposite the first base of a platinated GG site (23).

Additionally, we modelled **Benzi**TP in the active site of another thermostable A-family polymerase, *Bst* DNA Pol, for which a crystal structure is available with an incoming ddTTP opposite O^6-MeG (PDB code: 2HHW) (39). Furthermore, *Bst* DNA Pol has the closest amino acid sequence homology to *KlenTaq* polymerase with 51% identity matches (blastp against PDB protein database, http://www.ncbi.nlm.nih.gov/, 15/01/16) They share high sequence similarities in three conserved motifs among A-family DNA polymerases (Suplementary Figure S6A). The

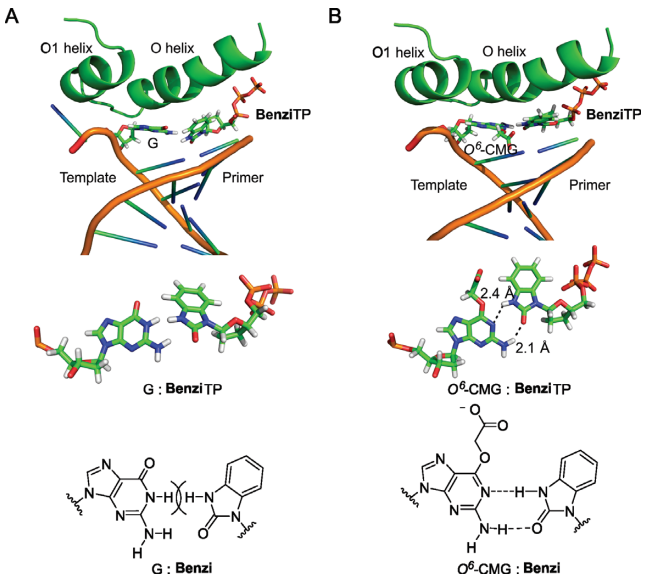

Figure 4. Molecular modeling of artificial **Benzi**TP opposite G (**A**) and O^6-CMG (**B**) template in the active site of *KlenTaq* mutant (M747K, I614K), PDB code: 3PY8 (33). Structures of possible base pairs between incoming **Benzi**TP and template G or O^6-CMG are given in the middle and at the bottom. DNA and polymerase O-helices are represented as cartoon, incoming **Benzi**TP and template base are visualized as sticks. Images were prepared using *PyMOL*.

structures were analyzed in the same manner described above, and the data indicate that **Benzi**TP is anticipated to be extruded approaching a pairing relationship with a template G and adopt a co-planar, two hydrogen bond, configuration when paired with O^6-MeG (Supplementary Figure S6B and C). The modeling results suggest the importance of hydrogen bonding interactions within the polymerase active site in explaining the experimental data.

Linear amplification of O^6-alkylG DNA

With the knowledge that **Benzi**TP specifically promotes full-length synthesis past O^6-CMG adducts, we further investigated whether adducted DNA could be linearly amplified using **Benzi**TP, which is specifically incorporated opposite O^6-alkylG as a marker for the adduct (Supplementary Figure S7A). Thus, to a low amount of O^6-CMG DNA (28 nt, X = O^6-CMG at position 24 nt, 0.5 ng DNA) was added four dNTPs plus **Benzi**TP and extension of a 19 nt primer to a full-length 28 nt product was monitored after 30 amplification cycles (95°C, 30 s; 42°C, 30 s; 55°C, 30 s) by

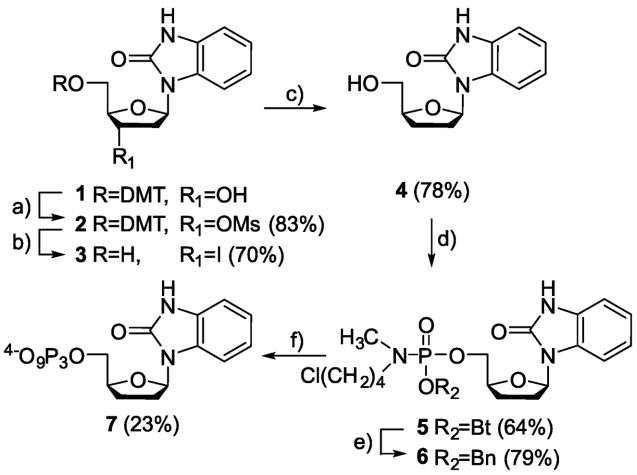

Scheme 1. Synthesis of 2′,3′-dideoxy **Benzi** nucleotide. (**a**) MsCl, Pyr, 0°C. (**b**) (i) NaI, DME, 90°C; (ii) DCA. (**c**) H_2, 10% Pd/C, MeOH. (**d**) (i) (4-chlorobutyl)(methyl)phosphoramidic dichloride, HOBt, THF, Pyr; (ii) NMI, THF. (**e**) BnOH, DMAP, THF. (**f**) (i) H_2, 10% Pd/C, DMF; (ii) PPi.

KTqM747K. Notably, with O^6-CMG template DNA, the addition of **Benzi**TP promoted formation of the 28 nt amplicon in 29-fold increased abundance relative to the template (SI, Figure S7B). However, with natural dNTPs only, an elongation product up to adduct site X was formed. In this study, we demonstrated successful linear amplification from biologically-relevant O^6-CMG DNA by *KTqM747K* DNA polymerase and **Benzi**TP whereby a labelled amplicon was generated that contains **Benzi** at the adduct site X in the original template, but with greater abundance than the original adduct.

Verification of Benzi incorporation opposite O^6-CMG adducts

In order to verify that **Benzi** is only incorporated opposite the O^6-alkylG adduct and not opposite canonical bases we performed a primer extension assay with a terminating **Benzi** nucleotide. This experiment required a 2′,3′-dideoxynucleoside analogue of **Benzi**TP, which was not previously reported. Thus, we prepared the base-modified 2′,3′-dideoxynucleoside-5′-*O*-triphosphate dd**Benzi**TP (Scheme 1). The **Benzi** nucleoside **1** (34) was mesylated at the 3′-position affording the respective 5′-*O*-dimethoxytrityl-3′-*O*-mesyl **Benzi** nucleoside **2** (49). Protected nucleoside **2** was allowed to react with sodium iodide, and the 5′-dimethoxytrityl group was removed with acid treatment, yielding the 3′-iodo derivative **3** (50). Elimination of the iodide from 3′-iodo **Benzi** nucleoside **3** by palladium-catalyzed hydrogenation yielded 2′-3′-dideoxy **Benzi** nucleoside **4** (50). Reaction with (4-chlorobutyl)(methyl)phosphoramidic dichloride gave rise to benzotriazole intermediate **5** (51,52), which following reaction with benzyl alcohol resulted in the phosphoramidate **6**. Next, monophosphate **6** was activated by catalytic hydrogenolysis with palladium on activated carbon. Filtration of the catalyst and subsequent addition of pyrophosphate resulted in formation of the desired triphosphate **7** (dd**Benzi**TP) (25).

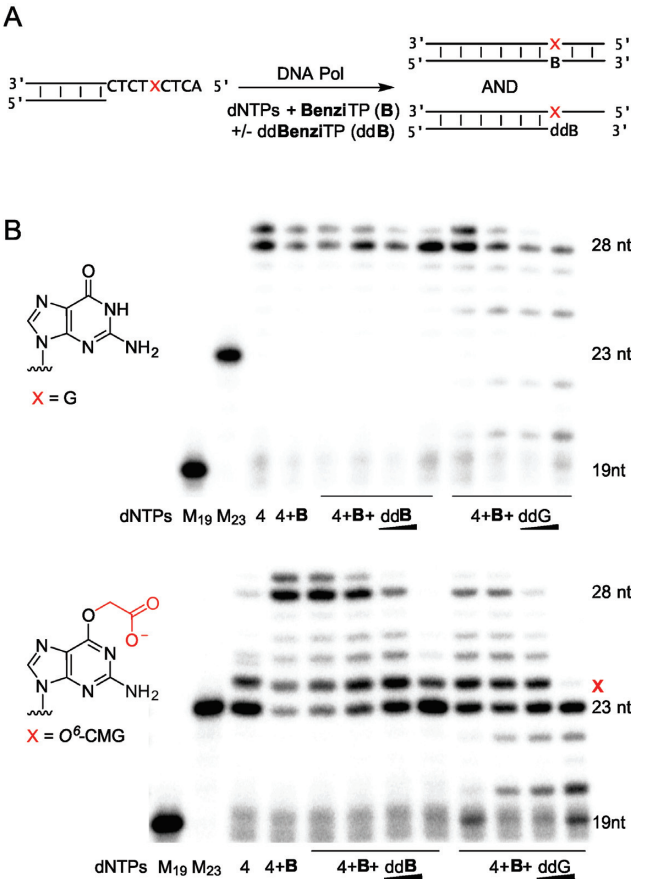

Figure 5. (**A**) Primer extension experiment with dd**Benzi**TP marking the position of O^6-CMG adduct in DNA by *KTqM747K* DNA polymerase. (**B**) PAGE analysis of reactions with DNA containing X = G or X = O^6-CMG at 24 nt using increasing concentrations of dd**Benzi**TP (0, 100, 500, 1000 and 2000 μM) added to 10 μM of all four natural dNTPs and 10 μM **Benzi**TP. M_{19}, primer 19 nt; M_{23}, 23 nt marker; 4, all four dNTPs; 4+**B**, all four dNTPs plus **Benzi**TP; 4+**B**+dd**B**, all four dNTPs, **Benzi**TP, plus dd**Benzi**TP; 4+**B**+ddG, all four dNTPs, **Benzi**TP, plus ddGTP.

With the newly synthesized dd**Benzi**TP at hand, we used it to test whether **Benzi** is exclusively incorporated opposite O^6-alkylG or if **Benzi** is also a substrate in replication of natural templates. Thus, templates containing G or O^6-CMG (28 nt, X at 24 nt) were annealed to a 19 nt primer and allowed to react with *KTqM747K* polymerase, in the presence of the four natural dNTPs (10 μM) and **Benzi**TP (10 μM) plus increasing concentrations of dd**Benzi**TP (Figure 5). In reactions containing template G, only desired full-length products were formed in the presence of four natural dNTPs, **Benzi**TP, and dd**Benzi**TP (Figure 5, X = G, 4+**B**+dd**B**). Hence, dd**Benzi**MP was not incorporated opposite canonical bases and did not impede DNA replication. As a positive control the same experiment was performed with ddG and the result was the appearance of bands at expected positions, i.e. from incorporation opposite templating C (Figure 5, X = G, 4+**B**+ddG). In replication of DNA containing O^6-CMG, adding increasing concentrations of dd**Benzi**TP to all four canonical dNTPs and **Benzi**TP resulted in a decrease of full-length products (band at 28 nt) and an increase in the band at the adduct site X

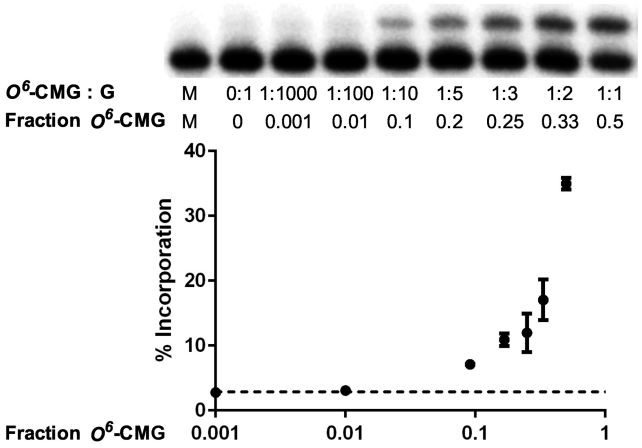

Figure 6. Recognition of DNA adduct in a mixture of O^6-alkylG- and G-containing oligonucleotides. Top: Primer extension reactions for O^6-CMG:G oligonucleotide mixtures (total concentration 22.5 μM template). Bottom: Percentages of *n+1* bands accounting for incorporation of **Benzi**MP (10 μM) incubated with corresponding O^6-CMG:G DNA mixtures (error bars represent standard error from triplicate measurements). Dashed horizontal line refers to background level from reactions that contained unmodified oligonucleotides only. Reactions were carried out at 55°C for 10 min.

(24 nt; Figure 5, X = O^6-CMG, 4+**B**+dd**B**). An additional band is visible at 23 nt, consistent with impeded incorporation of nucleotides opposite the O^6-CMG adduct due to polymerase stalling. Accordingly, this band is also observed in all other lanes. In control reactions, addition of ddG to all four dNTPs and **Benzi**TP resulted in bands at expected sites (Figure 5, X = O^6-CMG, 4+**B**+ddG). In reactions with template O^6-CMG containing the highest dd**Benzi**TP concentration (2000 μM), a band was visible at the adduct site X (24 nt; Figure 5B, X = O^6-CMG). This observation indicates that dd**Benzi**MP is specifically incorporated opposite O^6-CMG and can be used to directly mark the adduct site. In control reactions containing the highest amount of supplemented ddG, extension ended prior to the lesion (23 nt) resulting from O^6-CMG stalling *KTqM747K* polymerase. Thus, dd**Benzi**TP marked the O^6-CMG adduct specifically in the presence of natural dNTPs, further supporting the O^6-alkylG adduct-specific incorporation of **Benzi** and that the presence of the artificial nucleotide analogue does not perturb DNA replication by *KTqM747K* polymerase.

Recognition of O^6-alkylG adducts in DNA mixtures with unmodified templates

Knowing that **Benzi** is incorporated selectively opposite O^6-alkylG adducts, we examined whether the adducts could also be sensed in a mixture with non-damaged DNA. Thus, we performed a primer extension experiment with various dilutions of O^6-alkyl- and G-containing DNA (at a constant template concentration). Reactions were carried out with **Benzi**TP and *KTqM747K*, and the formation of *n* + 1 extension products was monitored (Figure 6). Reactions contained a 23 nt primer annealed to corresponding 28 nt templates with G or O^6-alkylG adducts at nucleotide 24. Concentration-dependent formation of extension products was observed that correlated with increasing fraction of O^6-alkylG present in a mixture with G templates (Figure 6, Supplementary Figure S8). For a 1:1 mixture of O^6-CMG:G DNA, 35% product was observed. In the absence of the O^6-CMG adduct, no extension product was formed (3%; Figure 6, dashed line). The lowest visually observable product (7%) was in the case of a 1:10 ratio of O^6-CMG:G. When the experiment was performed with O^6-MeG, 51% extension product was formed from a 1:1 mixture of O^6-MeG:G DNA, and the lowest detectable dilution was also 1:10 O^6-MeG:G (9%; Supplementary Figure S8). Critical limitations for addressing DNA adducts are that they exist at much lower levels and in the presence of a far larger excess unmodified DNA, as well as the lack of suitability of phosphorimaging as a basis of an optimized detection strategy. Nonetheless, the capacity for artificial nucleotide incorporation in a mixture was achieved, and furthermore, the amount of O^6-alkylG template present in the reactions, which corresponds to 0.17 ng O^6-alkylG DNA mixed with 1.7 ng unmodified DNA, was 3-fold lower than was detected by linear amplification (0.5 ng O^6-alkylG DNA; SI, Figure S7).

CONCLUSIONS

We investigated artificial nucleotides as substrates for the replication of DNA containing carcinogenic alkylation adducts O^6-MeG and O^6-CMG. We demonstrated that *KTqM747K* DNA polymerase specifically incorporated artificial nucleotide **Benzi**MP opposite O^6-MeG and O^6-CMG independent of its sequence context, and was competent in further extension. The specific incorporation of **Benzi**MP opposite O^6-alkylG adducts versus G was 150-fold higher for O^6-MeG, and 12-fold for O^6-CMG. O^6-MeG was readily bypassed by *KTqM747K* polymerase and full-length products were formed in the presence of natural dNTPs, whereas O^6-CMG stalled the polymerase and **Benzi**TP was required for efficient full-length DNA synthesis. A structural basis for O^6-alkylG adduct-specific incorporation of **Benzi** may be due to favorable hydrogen bonding interactions with O^6-alkylG while **Benzi** is extruded from the duplex when it is opposite G.

An additional advance described in this study was the preparation of the 2′,3′-dideoxynucleoside **Benzi**TP, which was used to mark the adduct site in O^6-CMG-containing DNA and confirm that **Benzi** is not incorporated opposite natural templates in full-length synthesis. This demonstration is the first example of an artificial dideoxynucleotide used in a sequencing experiment involving marking a DNA adduct site. The combination of artificial **Benzi**TP and *KTqM747K* polymerase allowed us to demonstrate a basis whereby O^6-alkylG adducts in mixtures with nondamaged G containing DNA may be sensed. While significant further adaptations for real biological applications, including enrichment strategies, sensitive analytical read-out methods, and further refinement of polymerase characteristics are needed, these findings are a chemical basis that suggest novel approaches for single-base resolution determination of mutagenic DNA adduct occurrence.

SUPPLEMENTARY DATA

Supplementary Data are available at NAR Online.

ACKNOWLEDGEMENT

We are grateful to Michael Raez (ETH Zurich, Switzerland) for preparing oligonucleotides containing O^6-CMG.

FUNDING

European Research Council [260341]; Swiss National Science Foundation [156280]; ETH research commission [ETH-43 14-1]. Funding for open access charge: ETH Zurich
Conflict of interest statement. None declared.

REFERENCES

1. Gates,K.S. (2009) An overview of chemical processes that damage cellular DNA: spontaneous hydrolysis, alkylation, and reactions with radicals. *Chem. Res. Toxicol.*, **22**, 1747–1760.
2. Fu,D., Calvo,J.A. and Samson,L.D. (2012) Balancing repair and tolerance of DNA damage caused by alkylating agents. *Nat. Rev. Cancer*, **12**, 104–120.
3. Pauly,G.T. and Moschel,R.C. (2001) Mutagenesis by O(6)-methyl-, O(6)-ethyl-, and O(6)-benzylguanine and O(4)-methylthymine in human cells: effects of O(6)-alkylguanine-DNA alkyltransferase and mismatch repair. *Chem. Res. Toxicol.*, **14**, 894–900.
4. Pence,M.G., Choi,J.Y., Egli,M. and Guengerich,F.P. (2010) Structural basis for proficient incorporation of dTTP opposite O6-methylguanine by human DNA polymerase iota. *J. Biol. Chem.*, **285**, 40666–40672.
5. Cancer Genome Atlas, N. (2012) Comprehensive molecular characterization of human colon and rectal cancer. *Nature*, **487**, 330–337.
6. Pfeifer,G.P., Denissenko,M.F., Olivier,M., Tretyakova,N., Hecht,S.S. and Hainaut,P. (2002) Tobacco smoke carcinogens, DNA damage and p53 mutations in smoking-associated cancers. *Oncogene*, **21**, 7435–7451.
7. Hecht,S.S. (2003) Tobacco carcinogens, their biomarkers and tobacco-induced cancer. *Nat. Rev. Cancer*, **3**, 733–744.
8. EUROGAST. (1994) O6-methylguanine in blood leucocyte DNA: an association with the geographic prevalence of gastric cancer and with low levels of serum pepsinogen A, a marker of severe chronic atrophic gastritis. The EUROGAST Study Group. *Carcinogenesis*, **15**, 1815–1820.
9. Hall,C.N., Badawi,A.F., O'Connor,P.J. and Saffhill,R. (1991) The detection of alkylation damage in the DNA of human gastrointestinal tissues. *Br. J. Cancer*, **64**, 59–63.
10. Lewin,M.H., Bailey,N., Bandaletova,T., Bowman,R., Cross,A.J., Pollock,J., Shuker,D.E. and Bingham,S.A. (2006) Red meat enhances the colonic formation of the DNA adduct O6-carboxymethyl guanine: implications for colorectal cancer risk. *Cancer. Res.*, **66**, 1859–1865.
11. Hecht,S.S. (1999) DNA adduct formation from tobacco-specific N-nitrosamines. *Mutat. Res.*, **424**, 127–142.
12. Rydberg,B. and Lindahl,T. (1982) Nonenzymatic methylation of DNA by the intracellular methyl group donor S-adenosyl-L-methionine is a potentially mutagenic reaction. *EMBO J.*, **1**, 211–216.
13. Middleton,M.R., Lee,S.M., Arance,A., Wood,M., Thatcher,N. and Margison,G.P. (2000) O6-methylguanine formation, repair protein depletion and clinical outcome with a 4 hr schedule of temozolomide in the treatment of advanced melanoma: results of a phase II study. *Int. J. Cancer*, **88**, 469–473.
14. Cupid,B.C., Zeng,Z., Singh,R. and Shuker,D.E. (2004) Detection of O6-carboxymethyl-2'-deoxyguanosine in DNA following reaction of nitric oxide with glycine and in human blood DNA using a quantitative immunoslot blot assay. *Chem. Res. Toxicol.*, **17**, 294–300.
15. Bouvard,V., Loomis,D., Guyton,K.Z., Grosse,Y., Ghissassi,F.E., Benbrahim-Tallaa,L., Guha,N., Mattock,H., Straif,K. and International Agency for Research on Cancer Monograph Working Group (2015) Carcinogenicity of consumption of red and processed meat. *Lancet Oncol.*, **16**, 1599–1600.
16. Himmelstein,M.W., Boogaard,P.J., Cadet,J., Farmer,P.B., Kim,J.H., Martin,E.A., Persaud,R. and Shuker,D.E. (2009) Creating context for the use of DNA adduct data in cancer risk assessment: II. Overview of methods of identification and quantitation of DNA damage. *Crit. Rev. Toxicol.*, **39**, 679–694.
17. Clark,T.A., Spittle,K.E., Turner,S.W. and Korlach,J. (2011) Direct detection and sequencing of damaged DNA bases. *Genome Integr.*, **2**, 10.
18. Riedl,J., Ding,Y., Fleming,A.M. and Burrows,C.J. (2015) Identification of DNA lesions using a third base pair for amplification and nanopore sequencing. *Nat. Commun.*, **6**, 8807.
19. Riedl,J., Fleming,A.M. and Burrows,C.J. (2016) Sequencing of DNA Lesions Facilitated by Site-Specific Excision via Base Excision Repair DNA Glycosylases Yielding Ligatable Gaps. *J. Am. Chem. Soc.*, **138**, 491–494.
20. Switzer,C.Y., Moroney,S.E. and Benner,S.A. (1993) Enzymatic recognition of the base pair between isocytidine and isoguanosine. *Biochemistry*, **32**, 10489–10496.
21. Matray,T.J. and Kool,E.T. (1999) A specific partner for abasic damage in DNA. *Nature*, **399**, 704–708.
22. Taniguchi,Y., Kikukawa,Y. and Sasaki,S. (2015) Discrimination between 8-oxo-2'-deoxyguanosine and 2'-deoxyguanosine in DNA by the single nucleotide primer extension reaction with Adap triphosphate. *Angew. Chem. Int. Ed. Engl.*, **54**, 5147–5151.
23. Nilforoushan,A., Furrer,A., Wyss,L.A., van Loon,B. and Sturla,S.J. (2015) Nucleotides with altered hydrogen bonding capacities impede human DNA polymerase eta by reducing synthesis in the presence of the major cisplatin DNA adduct. *J. Am. Chem. Soc.*, **137**, 4728–4734.
24. Stornetta,A., Angelov,T., Guengerich,F.P. and Sturla,S.J. (2013) Incorporation of nucleoside probes opposite O(6)-methylguanine by Sulfolobus solfataricus DNA polymerase Dpo4: importance of hydrogen bonding. *Chembiochem*, **14**, 1634–1639.
25. Wyss,L.A., Nilforoushan,A., Eichenseher,F., Suter,U., Blatter,N., Marx,A. and Sturla,S.J. (2015) Specific incorporation of an artificial nucleotide opposite a mutagenic DNA adduct by a DNA polymerase. *J. Am. Chem. Soc.*, **137**, 30–33.
26. Gong,J. and Sturla,S.J. (2007) A synthetic nucleoside probe that discerns a DNA adduct from unmodified DNA. *J. Am. Chem. Soc.*, **129**, 4882–4883.
27. Trantakis,I.A. and Sturla,S.J. (2014) Gold nanoprobes for detecting DNA adducts. *Chem. Commun.* , **50**, 15517–15520.
28. Trantakis,I.A., Nilforoushan,A., Dahlmann,H.A., Stauble,C.K. and Sturla,S.J. (2016) In-gene quantification of O6-methylguanine with elongated nucleoside analogues on gold nanoprobes. *J. Am. Chem. Soc.*, doi:10.1021/jacs.6b03599.
29. Gahlon,H.L., Boby,M.L. and Sturla,S.J. (2014) O6-alkylguanine postlesion DNA synthesis is correct with the right complement of hydrogen bonding. *ACS Chem. Biol.*, **9**, 2807–2814.
30. Gahlon,H.L., Schweizer,W.B. and Sturla,S.J. (2013) Tolerance of base pair size and shape in postlesion DNA synthesis. *J. Am. Chem. Soc.*, **135**, 6384–6387.
31. Peterson,L.A. (1997) N-Nitrosobenzylmethylamine is activated to a DNA benzylating agent in rats. *Chem. Res. Toxicol.*, **10**, 19–26.
32. Gloeckner,C., Sauter,K.B. and Marx,A. (2007) Evolving a thermostable DNA polymerase that amplifies from highly damaged templates. *Angew. Chem. Int. Ed. Engl.*, **46**, 3115–3117.
33. Obeid,S., Schnur,A., Gloeckner,C., Blatter,N., Welte,W., Diederichs,K. and Marx,A. (2011) Learning from directed evolution: Thermus aquaticus DNA polymerase mutants with translesion synthesis activity. *Chembiochem.*, **12**, 1574–1580.
34. Gahlon,H.L. and Sturla,S.J. (2013) Hydrogen bonding or stacking interactions in differentiating duplex stability in oligonucleotides containing synthetic nucleoside probes for alkylated DNA. *Chem. Eur. J.*, **19**, 11062–11067.
35. Raez,M.H., Dexter,H., Millington,C.L., van Loon,B., Williams,D.M. and Sturla,S.J. (2016) Translesion DNA synthesis past O6-carboxymethylguanine DNA by human Y- and B-Family polymerases promote error-free and error-prone bypass. *Chem. Res. Toxicol.*, **29**, in press.

36. Millington,C.L., Watson,A.J., Marriott,A.S., Margison,G.P., Povey,A.C. and Williams,D.M. (2012) Convenient and efficient syntheses of oligodeoxyribonucleotides containing O(6)-(carboxymethyl)guanine and O(6)-(4-oxo-4-(3-pyridyl)butyl)guanine. *Nucleos. Nucleot. Nucl.*, **31**, 328–338.
37. Boosalis,M.S., Petruska,J. and Goodman,M.F. (1987) DNA polymerase insertion fidelity. Gel assay for site-specific kinetics. *J. Biol. Chem.*, **262**, 14689–14696.
38. Creighton,S., Bloom,L.B. and Goodman,M.F. (1995) Gel fidelity assay measuring nucleotide misinsertion, exonucleolytic proofreading, and lesion bypass efficiencies. *Methods Enzymol.*, **262**, 232–256.
39. Warren,J.J., Forsberg,L.J. and Beese,L.S. (2006) The structural basis for the mutagenicity of O(6)-methyl-guanine lesions. *Proc. Natl. Acad. Sci. U.S.A.*, **103**, 19701–19706.
40. Tan,H.B., Swann,P.F. and Chance,E.M. (1994) Kinetic analysis of the coding properties of O6-methylguanine in DNA: the crucial role of the conformation of the phosphodiester bond. *Biochemistry*, **33**, 5335–5346.
41. Lim,S., Song,I., Guengerich,F.P. and Choi,J.Y. (2012) Effects of N(2)-alkylguanine, O(6)-alkylguanine, and abasic lesions on DNA binding and bypass synthesis by the euryarchaeal B-family DNA polymerase Vent (exo(-)). *Chem. Res. Toxicol.*, **25**, 1699–1707.
42. Chavarria,D., Ramos-Serrano,A., Hirao,I. and Berdis,A.J. (2011) Exploring the roles of nucleobase desolvation and shape complementarity during the misreplication of O(6)-methylguanine. *J. Mol. Biol.*, **412**, 325–339.
43. Woodside,A.M. and Guengerich,F.P. (2002) Effect of the O6 substituent on misincorporation kinetics catalyzed by DNA polymerases at O(6)-methylguanine and O(6)-benzylguanine. *Biochemistry*, **41**, 1027–1038.
44. Singer,B., Chavez,F., Goodman,M.F., Essigmann,J.M. and Dosanjh,M.K. (1989) Effect of 3' flanking neighbors on kinetics of pairing of dCTP or dTTP opposite O6-methylguanine in a defined primed oligonucleotide when Escherichia coli DNA polymerase I is used. *Proc. Natl. Acad. Sci. USA*, **86**, 8271–8274.
45. Singh,J., Su,L. and Snow,E.T. (1996) Replication across O6-methylguanine by human DNA polymerase beta in vitro. Insights into the futile cytotoxic repair and mutagenesis of O6-methylguanine. *J. Biol. Chem.*, **271**, 28391–28398.
46. Obeid,S., Blatter,N., Kranaster,R., Schnur,A., Diederichs,K., Welte,W. and Marx,A. (2010) Replication through an abasic DNA lesion: structural basis for adenine selectivity. *EMBO J.*, **29**, 1738–1747.
47. Eoff,R.L., Irimia,A., Egli,M. and Guengerich,F.P. (2007) Sulfolobus solfataricus DNA polymerase Dpo4 is partially inhibited by "wobble" pairing between O6-methylguanine and cytosine, but accurate bypass is preferred. *J. Biol. Chem.*, **282**, 1456–1467.
48. Choi,J.Y., Chowdhury,G., Zang,H., Angel,K.C., Vu,C.C., Peterson,L.A. and Guengerich,F.P. (2006) Translesion synthesis across O6-alkylguanine DNA adducts by recombinant human DNA polymerases. *J. Biol. Chem.*, **281**, 38244–38256.
49. Srivastav,N.C., Shakya,N., Mak,M., Agrawal,B., Tyrrell,D.L. and Kumar,R. (2010) Antiviral activity of various 1-(2'-deoxy-beta-D-lyxofuranosyl), 1-(2'-fluoro-beta-D-xylofuranosyl), 1-(3'-fluoro-beta-D-arabinofuranosyl), and 2'-fluoro-2',3'-didehydro-2',3'-dideoxyribose pyrimidine nucleoside analogues against duck hepatitis B virus (DHBV) and human hepatitis B virus (HBV) replication. *J. Med. Chem.*, **53**, 7156–7166.
50. Chu,C.K., Schinazi,R.F., Ahn,M.K., Ullas,G.V. and Gu,Z.P. (1989) Structure-activity relationships of pyrimidine nucleosides as antiviral agents for human immunodeficiency virus type 1 in peripheral blood mononuclear cells. *J. Med. Chem.*, **32**, 612–617.
51. Garrido-Hernandez,H., Moon,K.D., Geahlen,R.L. and Borch,R.F. (2006) Design and synthesis of phosphotyrosine peptidomimetic prodrugs. *J. Med. Chem.*, **49**, 3368–3376.
52. Tobias,S.C. and Borch,R.F. (2001) Synthesis and biological studies of novel nucleoside phosphoramidate prodrugs. *J. Med. Chem.*, **44**, 4475–4480.